

# AUTOMATIC 3D POWERLINE RECONSTRUCTION USING AIRBORNE LiDAR DATA

Y. Jwa, G. Sohn, H. B. Kim

GeoICT Lab, Earth and Space Science and Engineering Department, York University, 4700 Keele St., Toronto, ON M3J1P3, Canada  
– (yjwa, gsohn, hskim)@yorku.ca

Commission III WG 2

**KEYWORDS:** Corridor Mapping, LiDAR, 3D Reconstruction, Least-squared Adjustment, Perceptual Grouping, Risk Management

## ABSTRACT:

The safety of powerline infrastructure significantly affects our everyday life and industrial activities. There are many factors and objects to threaten powerline safety, which include encroaching vegetation, tree healthiness, ambient temperature of the powerlines, structural faults of insulator and tower and so on. A timely and accurate monitoring of those key powerline features enables to prevent causing possible dangerous situation such as blackout. At present, most of utility firms heavily rely on men-centric powerline monitoring methods which are time consuming and very costly, and also, hazardous work. Recently, airborne LiDAR system was introduced as a cost effective data acquisition tool which enables to rapidly capture 3D powerline scene with up to about 30 points/m<sup>2</sup>. This dramatically increased point density would provide a great possibility for achieving the automation of 3D reconstruction of powerline scene features which is an essential step for a machine-based powerline safety monitoring. Since it has been lately used for the powerline monitoring, not many automatic algorithms for reconstructing powerline have been introduced using LiDAR data. This paper introduces a Voxel-based Piece-wise Line Detector (VPLD) which automatically reconstructs 3D powerline models using airborne LiDAR data. The VPLD is developed based on well-known perceptual grouping framework which reconstructs a powerline by grouping similar features at different levels of information (i.e., points, segments and lines). A final reconstruction of single powerline models is accomplished by applying a non-linear adjustment for estimating catenary line parameters to a piece-wisely segmented voxel space. An evaluation of the proposed approach over a complicated powerline scene shows that the proposed method is promising.

## 1. INTRODUCTION

Powerline system conveys electric energy between networks of electric facilities to provide electricity to millions of homes and business. Electrical energy is transmitted through line conductors. In general, the line conductors can be categorized into three different types (i.e., transmission, sub-transmission and distribution) depending on its current capacity. Transmission line delivers high voltages from 69 kv to 765 kv and sub-transmission lines carry medium voltages from 34.5 kv to 69 kv. Distribution lines convey small voltages such as 7 kv and 13 kv due to distributing electric power to public customers (Kurtz et al., 1981). Canada's bulk transmission network consists of more than 160,000km of high voltage powerlines (Industry Canada, 2008), which contributes to the 2<sup>nd</sup> largest exporter of electricity and the fifth largest producer of electric power in the world. Since Canada experienced on the largest power outage: the Northeast Blackout of 2003, the importance of effective powerline system maintenance more increases along the corridor of land over which electric powerlines are located, called the Right-of-Way (ROW).

The management of powerline corridors is mainly focused on identifying and trimming hazardous trees which could fall and contact the powerline structure because the trees have large potential to cause power failures and a forest fire. Currently, most of utility companies endeavour to find the more cost-effective techniques to obtain clearances and improve access to the powerlines, which could be achieved by using the latest state-of-the-art passive and active remote sensing equipments such as digital camera and LiDAR system.

In recent years, dense 3D point clouds generated from LiDAR system with high range accuracy could provide easily 3D po-

werline models which are enable to extract semantic information with respect to powerline network system and vegetation located within ROW. In terms of industry needs, 3D model of the transmission line is required to monitor potentially dangerous situations like encroaching objects, and design and maintain the ROW. For example, based on 3D powerline models, vegetation management could be performed to keep clearance between conductor and vegetation by investigating conductor blowout according to the wind intensity and simulating the potential growth of trees. Thus, 3D powerline model can easily provide a multifaceted analysis for the risk management of power-line keeping safety and saving time and cost (Chaput, 2008).

This study is organized into six sections. Section 2 discusses the existing method for powerline reconstruction. In section 3, we introduce a new method for detecting and modeling powerlines based on non-linear adjustment computation. Section 4 presents the experimental result of the proposed technique's performance. Quality assessment for powerline modeling is provided in Section 5. Finally the paper will end with some concluding remarks and recommendations for future research.

## 2. PREVIOUS WORKS

For the last few decades, many research works concerning the detection and reconstruction of powerlines from airborne laser scanning point clouds and imagery has been conducted. Melzer and Briesse (2004) suggested a new method to reconstruct 3D powerlines using airborne LiDAR point clouds. In their method, fragmented powerline primitives were detected based on 2D Hough Transform from LiDAR data. A final powerline model

was reconstructed by estimating catenary line parameters with randomly selected line primitives based on RANSAC. Clode and Rottensteiner (2005) suggested a method to separate trees from powerlines using airborne LiDAR data. A stochastic decision on feature classification was made based on Dempster-Shafer's theory which combines multivariate properties extracted from LiDAR data. It was assumed that a significant height difference between first and last pulse return can be caused only from trees, powerlines and building edges. McLaughlin (2006) proposed a supervised knowledge-based classification method for differentiating powerlines from their surroundings. The developed technique showed successful classification results over high-voltage powerlines. They used airborne LiDAR data with the average point distance of from 1.2 to 2.4 meters on a powerline. Vale and Gomes-Mota (2007) addressed a new real time solution for data segmentation and anomaly identification algorithms using laser scanner attached to the helicopter fuselage. In each LiDAR sweep, the range data is classified into four different objects which include powerline, obstacles, tower, and ground. If geometrical mismatch happens due to variations of laser position, occlusions, and insufficient data resolution, line interpolation is processed by taking into account previous geometrical information.

The performance of algorithm for classifying and modeling powerline from laser point clouds usually depends on the quality of the LiDAR measurements derived from several factors such as position accuracy and point density. In general, point data with high point density can provide the robust result for detecting and segmenting transmission line because it is easy to apply various algorithms for classification. Thus, the usage of multi-return observations obtained from LiDAR system can contribute to a multifaceted analysis such as powerline network and vegetation analysis for transmission line maintenance and risk management, which triggers to automatically generate 3D model of powerline as well as tower. Currently, since the latest state-of-the-art laser scanner such as Riegl's LMS and Optech's ALTM series can provide full waveform measurement with high laser pulse repetition rates, about 160 kHz, a lot of target echoes can be introduced by waveform digitizer.

### 3. APPROACH AND METHODOLOGY

The detection and modeling of powerline is performed under the assumption that transmission line always hangs over terrain at the certain height and is not disconnected within one span. The direction of powerline is also not changed abruptly within span and tower is located around the intersection of lines in between spans.

The powerline points are detected based on perceptual grouping framework related to Gestalt laws of perceptual organization which is extracting relevant groupings and structures from irregularly distributed points, fragments, and segmenting elements sharing similar characteristics. Output of each process step becomes input to the next step. For example, powerline candidate points, which are detected from unclassified LiDAR data, are used to cluster powerline points situated around the candidate points as line fragments which, in turn, will be meaningful semantic information to extract single powerlines. We use several criteria of perceptual organization for extracting and modeling power-line as follows:

- Similarity : neighbour powerline closely located each other can be separated using similar linear property in local searching region

- Proximity : powerline points can be grouped as the same cluster by gathering points according to the direction of each powerline
- Continuity : powerline can be modelled based on catenary curve using continuously distributed powerline points

Figure 1 illustrates the work flow for powerline detection and modeling based on perceptual grouping framework which consists of three information levels: point, fragment, and line.

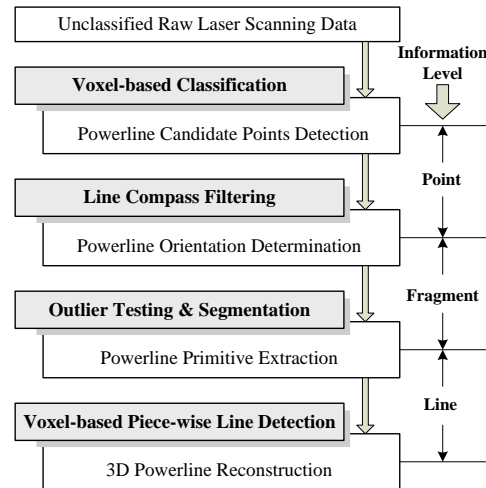


Figure 1. The work flow for powerline reconstruction based on perceptual grouping framework

#### 3.1 Powerline Candidate Points Detection

The first step for reconstructing powerlines is to extract a powerline candidate point that indicates a possible presence of powerlines. This step would be greatly helpful for reducing scene complexity so that the remaining reconstruction tasks can focus on only smaller numbers of points. In other words, main aid of the first step is to derive the linear features perceived to be the power lines. The input points are subdivided by voxel space where each voxel has the same size (5m X 5m X 5m). The voxel size is determined by the span between each powerline. Several approaches for separation of cables from non-cables were investigated. One of the applied methods is Hough-Transform, which is a well-known algorithm to detect linear features in image processing. However, the method needs to be enhanced for applying 2D projected LiDAR points per voxel to Hough-Transform. In addition, powerline points are not placed on an ideal line, so the Hough space graph does not intersect in one bin after  $(x, y)$  plane to  $(r, \theta)$  plane conversion. Therefore, 8 neighborhoods as well as the bin with the highest count in the accumulator space are taken into account. When the index of the bin with the highest count is  $(j, k)$  in  $i^{\text{th}}$  voxel, the discriminator of Hough-Transform is defined by:

$$D_{Hough} = \frac{\sum_{p=j-1}^{j+1} \sum_{q=k-1}^{k+1} h_{(p,q)}}{N_i} \quad (1)$$

where  $h_{(p,q)}$  is the count at the bin  $(p, q)$  and  $N_i$  is the number of points within the  $i^{\text{th}}$  voxel. The second method is Eigenvalue, which is determined by the eigen decomposition for a set of 3-D points. Supposed the computed eigenvalues are  $\lambda_0, \lambda_1,$  and  $\lambda_2$ ,  $\lambda_0$  is much larger than the others in case of linear feature. Thus, the ratio of  $\lambda_0$  to the difference between  $\lambda_1$  and  $\lambda_2$  is applied to detect linear features from point sets. An extensive experiment

proved that the computation of Eigenvalue ratio is much faster than Hough-Transformation. However, in case which two wires are located very closely, it becomes more difficult to separate them each other. A density of points within a voxel is also taken into consideration since a voxel which includes points regarded as the components of powerlines and located in the air has low point density. In practice, the optimal thresholds of three factors are derived by training several samples. Finally, the LiDAR points are separated by the rule-based classification considering Hough-Transform, Eigenvalue, and point density. Figure 2 shows a work flow for classifying point clouds within a voxel into three classes including linear, non-linear, or undefined feature using a combination of three factors. The unclassified features corresponding to powerlines are tackled in the next step: Powerline Primitive Extraction.

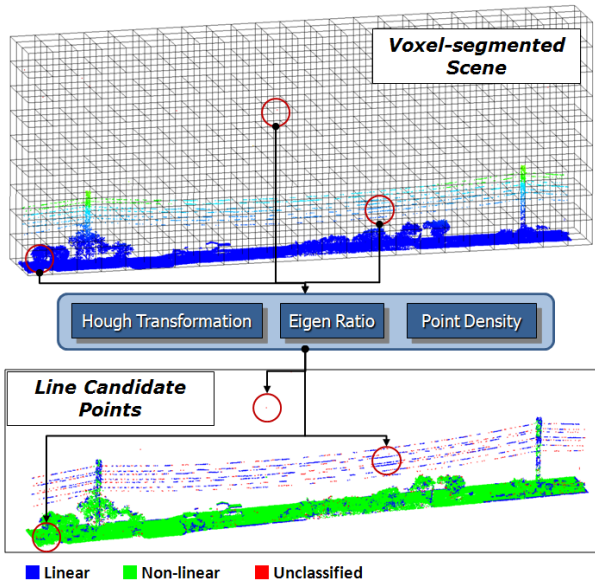


Figure 2. Illustration of a 3D voxel-based classification of powerline candidate points.

### 3.2 Powerline Orientation Determination

After extracting powerline candidate points, an initial orientation angle of powerlines is determined over each candidate point. For achieving this goal, a Compass Line Filter (CLF) is applied as suggested by Sohn et al (2007). The CLF is designed as a set of eight line directions spaced with equally 22.5°, the initial powerline direction is assumed to consist of eight directions, and one of eight hypotheses (H) is allocated into each powerline candidate point within user-driven cubic searching area. For each hypothesis of eight line directions,  $\Omega$ , which is the sum of the squared residuals between hypothesis and observations, is calculated for model closeness using line equation  $d = x \cos \theta + y \sin \theta$ , where  $\theta$  indicates the angle between a line segment and  $x$ -axis and  $d$  is the distance from the origin, and hypothesis (H\*) with minimum  $\Omega$  is selected as initial line direction at the current powerline candidate point. Given a hypothesis, H, and model suitability,  $\Omega$ , H\* is now defined as

$$H^* = \min_{\forall(H)}(\Omega) \quad (2)$$

Figure 3 illustrates the suggested method for determining a powerline orientation using powerline candidate points detected in section 3.1. In figure 3, a line direction index of eight (8) is fi-

nally chosen as its initial powerline orientation since it shows the minimum residuals between a hypothesized line filter and powerline candidate points. This process applies to all the powerline candidate points which serve as a similarity cue for grouping as powerline fragment.

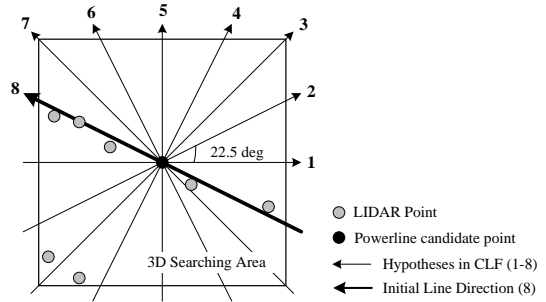


Figure 3. An illustration of powerline initial orientation determination at the powerline candidate point based on CLF.

### 3.3 Powerline Primitive Extraction

The first task in this step is to sort powerline candidate points according to  $\Omega$  in Eq. (1), since the initial direction of powerline point with minimum  $\Omega$  is close to the real direction of powerline. In the local searching region, it is possible to make assumption that the powerline can be expressed as line with linear property. Thus, based on a line equation in the horizontal and vertical domain, outlier testing with F distribution can be performed to extract powerline primitive and separate closely distributed powerline primitives.

The test statistic T for outlier testing can be as following form:

$$T_j = \frac{(\tilde{\epsilon}_j)^2 \frac{P_j}{r_j}}{\left[ \hat{\sigma}_0^2(n-m) - (\tilde{\epsilon}_j)^2 \frac{P_j}{r_j} \right] / (n-m-1)} \quad (3)$$

$\sim F(1, n-m-1)$  under  $H_0$

Where, the subscript  $j$  indicates for LiDAR point;  $n$  and  $m$  are the number of observation and parameter, respectively;  $r_j = (Q_{\tilde{\epsilon}} P)_{jj}$  is reliability for detecting gross errors;  $Q_{\tilde{\epsilon}} = P^{-1} - AN^{-1}A^T$ ,  $\hat{\sigma}_0^2 = (n-m)^{-1}(\tilde{\epsilon}^T P \tilde{\epsilon})$

For each domain, the procedure for line segmentation is as follows:

- In the horizontal domain, test statistic T values for each point within searching area are calculated to obtain the rough range of critical value for F distribution within small sub-searching area around current powerline candidate point along initial powerline direction.
- Hypothesis testing for outliers to each LiDAR point located in 3D searching area is carried out within the range of critical value.
- LiDAR points satisfying with null hypothesis are allocated into the same powerline group.
- In the vertical domain, the procedure of height clustering is performed based on outlier testing, and each group is divided into sub-clusters as the above steps.
- Finally, the accurate powerline direction for each group is calculated by using member points and a new sub-cubic box

including member points is generated to be used as a priori information for the next step.

Figure 4 shows powerline primitive extraction derived from powerline candidate points based on outlier testing in 3D searching area. The new sub-cubic box is generated with three factors: length, width and height. Length factor as user-driven value is determined taking into account the average distance of powerline point. Width and height factors are computed based on the distribution of powerline points.

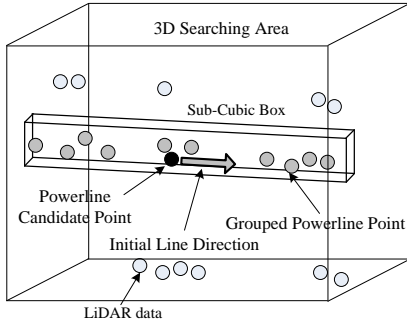


Figure 4. Powerline primitive extraction based on outlier testing in a cubic searching region

### 3.4 3D Powerline Reconstruction

A powerline primitive has information on initial line direction, powerline member points and a sub-cubic box as explained in the powerline primitive extraction step. Where, the sub-cubic box is called voxel generated for Grouping (VG) from this section. In this section, the grouping process of powerline point from the line fragment is discussed in detail. We propose a new method to detect and group powerline points, called Voxel-based Piece-wise Line Detector (VPLD), which continuously generates 3D cubic searching area based on a priori information such as parameters of catenary curve equation and VG, and dynamically detects LiDAR points located on the same power line and estimates accurate parameters consisting of current VG. The derived equation of catenary curve from the basic form in Cartesian coordinates is described by the following equation.

$$z = a + (c + c_1) \cosh\left(\frac{x_{or}y - b}{c + c_1}\right) + a_1 \quad (4)$$

Where,  $a$  and  $b$  are parameters for translation of the origin;  $c$  is a scaling factor denoted as the ratio between the tension and the weight of the hanging flexible wire per unit of length;  $c_1$  and  $a_1$  are additional parameters for propagating voxels along powerline points.

Based on VPLD using catenary curve, powerline can be clustered and modeled at the same time using stochastic process by measurement update and parameter prediction step, iteratively, as shown in Figure 5.

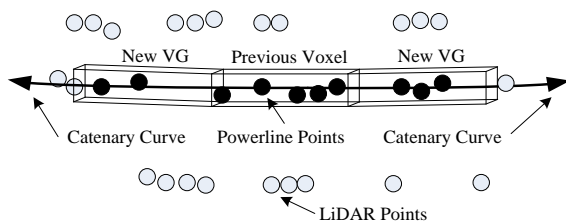


Figure 5. VPLD procedure based on catenary curve equation

In each voxel, the algorithm for detecting and grouping powerline point is described as follows in detail.

- A new VG is generated according to catenary curve introduced from the previous VG and LiDAR points existed in the new VG is allocated as powerline points on the same line.
- Parameters consisting of catenary equation and new VG are ratified by using new observations.
- The above steps, first and second, are processed, iteratively until the shape of detected powerline will be symmetric form.
- VGs at the left and right side of detected powerline are propagated, continuously, based on first and second step at the same time taking into account the stop condition of VPLD procedure

VPLD process will be stopped by checking  $c_1$  variation as shown in Figure 6. That is, if the variation of  $c_1$  value calculating from difference between previous and current VG converges into less than  $\epsilon$  which is user-driven small value, the procedure will be ended.

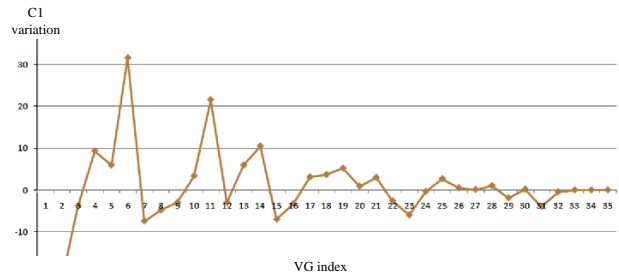


Figure 6.  $c_1$  variation in accordance with VG index

The main advantage of VPLD system can be to apply to the target area with low point density and possible to separate powerlines located on close to each other because estimated catenary curve can play a role of guideline. In case observations, which are LiDAR points in the same group, are not enough for adjusting parameters of catenary curve equation, new voxel will be generated by using line equation instead of catenary curve equation.

## 4. EXPERIMENTAL RESULT

The test data set, which is depicted in Figure 7(a), was captured over urban with crossing area in east of Folsom, California, USA on Aug., which covers an area of about 2094(length)×385(width)  $m^2$  and height range from 31 to 171 meters using Riegl Q560 laser scanner attached helicopter with about 400 meters flight height. We collected 1.8 million laser points at the average point density of 5 (points/ $m^2$ ) and average point distance on powerline of 1 meter. Multiple returns from a single shot were recorded to increase point density on the transmission line.

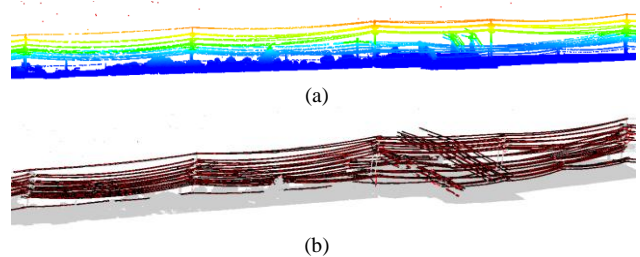


Figure 7. Test data set (a) and extracted powerline models (b)

We counted total 112 numbers of powerline located in 7 spans and distributed toward length direction in the target area. Table 1 shows the result of powerline extraction in the line modeling level. The result illustrates VPLD approach comparatively provides a robust solution with about 93.8% success rate to completely model transmission lines. However, partial detected powerlines occur in case that powerline passes through vegetation and powerline points are sparsely distributed at the lower height. In case of un-detected part, as powerline points with low point density can be grouped as other object, the powerline cannot be extracted in the VPLD process.

Table 1. The result of powerline extraction in the line modeling level

	Complete detection	Partial detection	Undetected
Number	105	5	2
Rate (%)	93.8	4.5	1.7

### 5. QUALITY ANALYSIS

In order to achieve effective evaluation for our approach, we choose three types of span with respect to scene complexity.

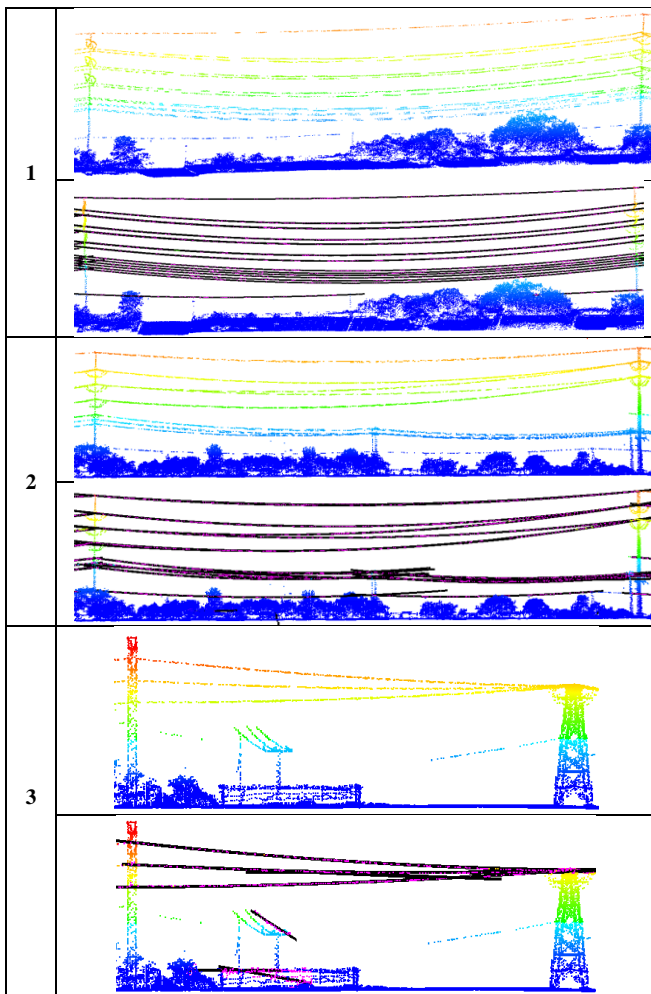


Figure 8. Three categories' data set in urban target area

Figure 8 shows graphically unclassified LiDAR data and the result of powerline modeling according to each category. Power-

line structure in site 1 has complicate structure including distribute over residence area and one line with low height is passing through vegetation. We can also find less than 1 meter closely located two lines in six pair's lines. In site 2, there are transmission, subtransmission, and distribution lines over vegetation area, and two lines in the top diverge. Powerlines with very strong linear property is depicted in site 3.

Success rate for each site is listed in Table 2. The results illustrate complete success rate in most selected site indicates high percentage. The partial detection usually occurs in the powerline with low point density because VPLD process is terminated early due to sparsely distributed observations, and in the powerline passing through vegetation. Therefore, point density on the powerline and obstacles can mainly contribute to the modeling process.

Table 2. The result of powerline extraction in each category

site	Size (meter)	#Line	Complete	Partial	Un-detected
1	645(L) × 57(W)	21	20	1	0
2	728(L) × 78(W)	28	28	0	0
3	242(L) × 96(W)	6	4	2	0

Figure 9 shows deviation in Cartesian coordinates between powerline models and powerline points according to three selected site. Average 3D deviation is less than 25 cm which shows good powerline modeling if 3D accuracy of about 30 cm on LiDAR data is taken into account.

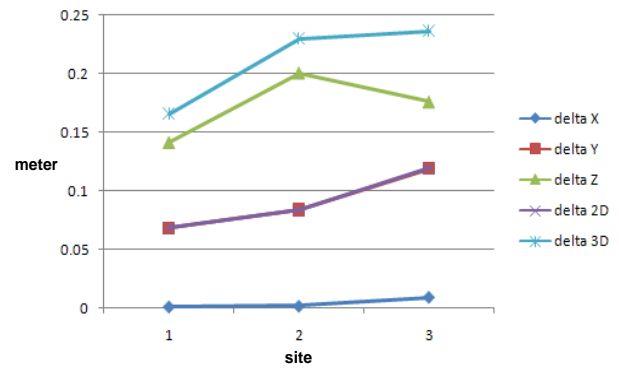


Figure 9. Deviation between powerline models and powerline points in three categories' data set

### 5. CONCLUSIONS

This study presented the new method, VPLD, for automatic reconstruction of powerline model using only irregular distributed laser scanning data without the existing data base information such as tower position and the number of line. VPLD was processed by dynamically generating piece-wise VG and detecting powerline points, and then reconstructing powerline models based on a non-linear adjustment of catenary lines.

The experiment shows that the proposed VPLD approach can achieve 93.8 % success rate for extracting powerlines from unclassified LiDAR data set with an average point distance of 1.4 meters on the powerlines. The VPLD shows that it can achieve both detection and modeling of powerline at the same time by iteratively update and prediction of catenary line parameters based on a stochastic manner. In the future, the proposed method will be applied to large-scale urban and rural data set, and integrates with the module of tower detection and modeling.

Furthermore, we will investigate algorithms for detecting individual insulator's position and deriving deflection and temperature of powerlines based on catenary line parameters estimated

### ACKNOWLEDGMENTS

This research was supported by a grant from project titled "Automated Change Detection of 3D Landscape Objects for Powerline Corridor Mapping by Integrating Airborne LiDAR and Multiple-viewing Digital Cameras" funded by Ontario Centres of Excellence and GeoDigital International Inc.

### REFERENCE

Chaput, L.J., 2008. Understanding LiDAR data – How Utilities can get Maximum Benefits from 3D Modeling, *International LiDAR Mapping Forum (ILMF) 2008*, Denver, CO, USA, Feb. 21-22, (On CD-ROM).

Clode, S. and Rottensteiner, F., 2005. Classification of Trees and Powerlines from Medium Resolution Airborne Laserscanner Data in Urban Environments, In: *Proceedings of APRS Workshop on Digital Image Computing 2005 (WDIC2005)*, Brisbane, Australia. (On CD-ROM).

Eckert, K., 2004. Proper Tree and Vegetation Management Makes Major Differences. *Natural Gas Electricity*, Vol. 21(5), pp. 1-8.

Ituen, I. and Sohn, G., 2009. The Way Forward: Advanced in Maintaining Right-Of-Way of Transmission Lines, *GEOMATICA. Submitted*.

Kurtz, E. B., Shoemaker T. M., 1981. The lineman's and cableman's handbook, 6<sup>th</sup> edition, New York

Lu, M.L. and Kieloch, Z., 2008. Accuracy of Transmission Line Modeling Based on Aerial LiDAR Survey, *IEEE Transactions on Power Delivery*, Vol. 23, pp. 1655-1663

McLaughlin, R. A., 2006. Extracting Transmission Lines From Airborne LIDAR Data, *IEEE Geoscience and Remote Sensing Letters*, Vol. 3, NO. 2, pp. 222-226.

Melzer, T. and Briese, C., 2004. Extraction and Modeling of Power Lines from ALS Point Clouds, In: *Proceedings of 28<sup>th</sup> Austrian Assoc. Pattern Recog. Workshop*, Hagenberg, Austria, Jun. 17-18, pp. 47-54.

Sarabandi, K. and Park M., 2000. Extraction of Power Line Maps from Millimeter-Wave Polarimetric SAR Images. *IEEE Transactions on Antennas and Propagation*, Vol. 48, No. 12, pp. 1802-1809.

Sohn, G. and Dowman, I., 2007. Data fusion of high-resolution satellite imagery and LiDAR data for automatic building extraction. *ISPRS Journal of Photogrammetry and Remote Sensing*, 62(1), pp. 43-63

Vale, A. and Gomes-Mota, J., 2007. LIDAR Data Segmentation for Track Clearance Anomaly Detection on Over-head Power Lines, In: *Proceedings of IFAC Workshop*, Turkey, pp. 17-19